Polymer Chemistry

Accepted Manuscript

This article can be cited before page numbers have been issued, to do this please use: A. V. Galukhin, I. Nikolaev, R. V. Nosov and S. Vyazovkin, *Polym. Chem.*, 2020, DOI: 10.1039/D0PY00554A.

View Article Online
DOI: 10.1039/D0PY00554A

ARTICLE

Solid-state polymerization of a novel cyanate ester based on 4-*tert*-butylcalix[6]arene

Received 00th January 20xx,
Accepted 00th January 20xx

DOI: 10.1039/x0xx00000x

Andrey Galukhin,[a*] Ilya Nikolaev,[a] Roman Nosov,[a] Sergey Vyazovkin[a,b*]

A unique cyanate ester based on 4-*tert*-butylcalix[6]arene has been synthesized. It melts above 400°C and polymerizes on heating above 300°C, i.e., in the solid state. The techniques of FTIR, pXRD, NMR, MALDI, TGA, DSC, and fast scanning chip-calorimetry have been used to characterize the monomer and its polymerization. The kinetics of solid-state polymerization has been analyzed by an advanced isoconversional method that has revealed that the process rate is limited by a single step. The activation energy of the process has demonstrated unusually large value, 380±10 kJ mol^{-1}, which points at cooperative breaking of C≡N bonds as the rate limiting step. This is in contrast to the regular cyanate esters that polymerize in the liquid-state by consecutive breaking of C≡N bonds. It has also been found that polymerization follows zero-order kinetics, which is explained by the topochemical nature of polymerization localized on the surface of the plate-like crystals of the monomer.

Introduction

Solid-state polymerization (SSP) is a powerful tool for creating polymers with controllable structure, molecular weight, molecular weight distribution, tacticity, etc.[1-3] SSP can proceed both in crystalline and amorphous state. The polymerization in crystalline state affords synthesis of highly ordered polymers with unique optoelectronic properties,[4-7] whereas polymerization of starting material in amorphous state (in the temperature range between the glass transition and melting temperatures) allows to obtain polymers of high molecular weight,[8-12] which are unavailable by polymerization in a melt because of the problems with extremely high viscosity of the products and their degradation at higher temperatures.[13] In addition to practical advantages, SSP is of fundamental interest.[14] Among important fundamental issues is obtaining insights in how the mobility of monomer or oligomer molecules and their preorganization in the solid state affect the mechanism and kinetics of polymerization as well as the structure of a forming polymer. For instance, studies of solid-state [2+2] polycycloaddition of diolefins,[4] and SSP of diacytelenes[5-7,15] have shed some light on the crystal lattice control of the reaction kinetics and developed the strategies for overcoming an unfavorable orientation of the crystal lattice molecules by introducing specific substituents or auxiliary components.[16]

To the best of our knowledge, neither thermal nor photo initiated SSP has been reported for cyanate esters. This is not surprising considering their reactivity. Initiation of cyanate esters polymerization requires rather high temperatures, typically above 200 °C, so that they melt before the reaction starts.[17] The mechanism of the liquid-state polymerization of cyanate esters includes consecutive addition of three monomer molecules followed by cyclization (Figure 1).[18] Such sequence of reactions is unlikely in the solid state because of restricted mobility of the monomer molecules. Thus, one can hypothesize that the solid-state polymerization of cyanate esters, if possible, should demonstrate the mechanism and kinetics that are distinctly different those observed in the liquid-state.

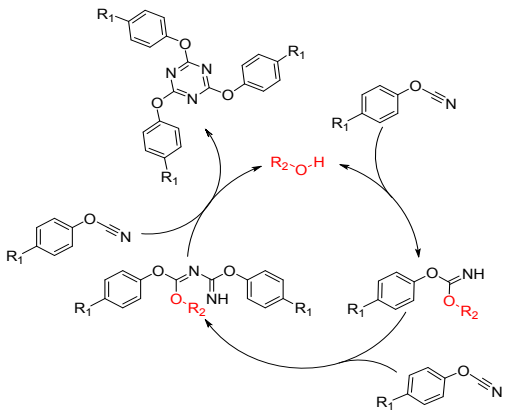

Figure 1. Mechanism of cyclotrimerization of cyanate esters.

In order to test this hypothesis, we have synthesized cyanate ester monomer based on 4-*tert*-butylcalix[6]arene. Since the corresponding precursor, 4-*tert*-butylcalix[6]arene,

[a]*Alexander Butlerov Institute of Chemistry, Kazan Federal University, 18 Kremlevskaya Street, Kazan 420008, Russian Federation*
[b]*Department of Chemistry, University of Alabama at Birmingham, 901 S. 14th Street, Birmingham, AL 35294*

Electronic Supplementary Information (ESI) available: Single crystal of the monomer placed on chip-sensor (Figure S1), ^{1}H, ^{13}C NMR, and MALDI spectra of monomer (Figures S2-S4), SEM image of monomer aggregated crystals (Figure S5), ESI mass-spectrum of gas mixture evolved during polymerization (Figure S6), FSC curve of monomer melting, and plots of variation of melting temperatures with heating rates (Figures S7 and S8). See DOI: 10.1039/x0xx00000x

melts around 370°C,[19] it was expected that the synthesized monomer would melt at high temperature and, thus, polymerize in the solid state. Our expectations have been confirmed experimentally, presenting what appears to be the first known case of solid-state polymerization of cyanate esters. The kinetics of the solid-state polymerization has been studied by differential scanning calorimetry (DSC) and analyzed by means of isoconversional methodology.[20] The kinetic analysis has revealed two remarkable phenomena for the solid-state polymerization of the synthesized cyanate ester. The first one is an unusually large activation energy of the process. The second is the zero-order kinetics, which, to the best of our knowledge, has never been reported for solid-state polymerization. The paper is focused on providing physical insights into both phenomena.

Materials and methods

4-*tert*-butylphenol (99 %, Aldrich Chemistry), potassium hydroxide (>98 %, ChemMed), formaldehyde (37.5 w.% solution in water, Fisher Scientific), p-xylene (>98 % TatChemProduct), triethylamine (>99%, Sigma-Aldrich), cyanogen bromide (97%, Acros Organics), trichlormethane (>99.5%, ChemMed), acetone (>98%, TatChemProduct) were purchased and used as received. Tetrahydrofuran (THF, >98 %, ChemMed) was purchase and additionally distilled over potassium hydroxide. 4-*tert*-butylcalix[6]arene was synthesized according to the literature procedure.[19] Scheme of synthesis of cyanate ester monomer presented in Figure 2.

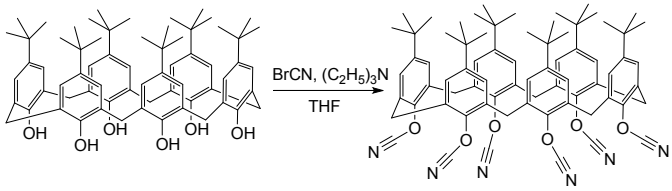

Figure 2. Scheme of synthesis of cyanate ester monomer from 4-*tert*-butylcalix[6]arene.

NMR spectra were recorded on Bruker Avance-400 spectrometer at 400 MHz for ^{1}H, and 100 MHz for ^{13}C with $CDCl_3$ as a solvent. Chemical shifts are reported in delta (δ) units in parts per million (ppm). FTIR spectra were recorded with Bruker Vertex 70 FTIR spectrometer. MALDI spectra were recorded by Bruker autoflex speed mass-spectrometer using 2,5-dihydroxybenzoic acid as the matrix. DSC runs were carried out using a heat flux DSC (Mettler-Toledo, DSC 3+). Indium and zinc standards were used to perform temperature, heat flow, and tau-lag calibrations. Solid state polymerization was carried out in situ in 40 µL aluminium DSC pans. Non-isothermal DSC runs were performed at the heating rates of 2.5, 5.0, 7.5, 10.0, 12.5, and 15°C min^{-1}. Isothermal DSC run was performed at 338 °C. This temperature was selected to be roughly around the temperature at which polymerization becomes detectable at the slower heating rates (2.5 - 5.0°C min^{-1}). The target isothermal temperature was reached at the heating rate 30 °C min^{-1}. The use of the faster heating rate guaranteed that no appreciable polymerization would occur before the target temperature was reached. The isothermal and nonisothermal DSC runs were performed in the atmosphere of argon flow at 80 mL min^{-1}, as recommended by the manufacturer (Mettler-Toledo). Because moisture could potentially affect polymerization, the monomer was placed in 40 µL aluminum pans and kept in a vacuum desiccator containing P_2O_5 for 1 day to remove traces of water before measurements. For measurements, the pans were closed with pierced lids to avoid the pressure build-up and potential bursting of the pans. Simultaneous TGA - DSC runs were carried out with Netzsch STA 449 F1 Jupiter thermal analyzer. The experiments were conducted with the same heating rates as for the DSC runs under argon flow of 75 mL min^{-1}, as recommended by the manufacturer (Netzsch). The mass of the sample for all thermal analysis runs was ~1-2 mg. A fast scanning calorimeter Flash DSC 1 (Mettler Toledo) was used for determination of the monomer melting temperature. In this experiment, a single crystal of the monomer was picked by a 30 µm copper wire from a bulk sample with the help of a LEICA M60 optical microscope, placed in the centre of 157 × 157 µm area of the MultiSTAR UFS 1 MEMS chip sensor (See Figure S1 in SI), and heated at the rates of 6 000 – 60 000 °C min^{-1}. The measuring cell was continuously purged with argon at 40 mL min^{-1}.

Synthesis of cyanate ester monomer. In a 250 mL three neck round bottom flask equipped with magnetic stirrer and two dropping funnels, the solution of 1.62 g (15.4 mmol) of cyanogen bromide in 30 mL of THF was placed and cooled to −40 °C. Then one dropping funnel was filled with a solution of 0.50 g (0.51 mmol) of 4-*tert*-butylcalix[6]arene in 30 mL of THF. Other one was filled with a solution of 1.9 mL (13.9 mmol) of triethylamine in 30 mL of THF. Both solutions were added dropwise to the reaction mixture during 1 hour. After that the mixture was stirred for 1 h more at a temperature of −30 °C. Then triethylammonium bromide salt was filtered off and solvent was evaporated. Yellow residue was washed with several portions of acetone and recrystallized from trichloromethane. Desired cyanate ester monomer was obtained as a white solid with a yield of 73% (0.42 g). FTIR: 2360, 2265 cm^{-1} (-OCN). ^{1}H-NMR, $CDCl_3$-d1, δ (ppm): 1.19 (s, 54H, $(CH_3)_3C$), 4.16 (s, 12H, $(-CH_2)$), 7.09 (s, 12H, Ar-H). ^{13}C-NMR, δ (ppm): 151.68, 148.36, 129.40, 127.54, 109.60, 34.62, 31.19, 31.03 (Figures S2 and S3 in SI). MALDI–TOF MS (2,5-dihydroxybenzoic acid was used as a matrix) analysis (Figure S4 in SI) revealed two major peaks at m/z = 1146.4 and 1162.5 corresponding respectively to the $[M+Na]^+$ and $[M+K]^+$ adducts. A very minor peak at m/z = 1186.4 was assigned to $[M+Cu]^+$. All these peaks were consistent with the calculated mass for M ($C_{72}H_{78}N_6O_6$) is 1123.4. A few other minor peaks at smaller m/z correspond to partially substituted derivatives of 4-*tert*-butylcalix[6]arene. Elemental analysis for ($C_{72}H_{78}N_6O_6$).

View Article Online
DOI: 10.1039/D0PY00554A

Calculated (%): C, 76.98%, H, 7.00%, N, 7.48%. Found (%): C, 77.12%, H, 6.94%, N, 7.58%.

Computations

The recommendations of the ICTAC Kinetic Committee[21] were followed to evaluate the activation energy, preexponential factor, and the reaction model of the studied processes. The extent of conversion, α, values were determined as the partial areas of the DSC peaks associated with polymerization of the cyanate ester. The effective activation energy, E_α, was evaluated as a function of conversion with the aid of the flexible integral isoconversional method of Vyazovkin, which allows to eliminate a systematic error in E_α when it varies with α.[22-25] The error is eliminated by using the so-called flexible integration that assumes the constancy of E_α within a very narrow integration range, Δα.[20,25] The value of Δα was taken as 0.02. Within each Δα, E_α is determined by finding a minimum of the function:

$$\Phi(E_\alpha) = \sum_{i=1}^{n}\sum_{j\neq i}^{n}\frac{[I(E_\alpha, T_{\alpha,i})\beta_j]}{[I(E_\alpha, T_{\alpha,j})\beta_i]} \quad (1)$$

where

$$I(E_\alpha, T_{\alpha,i}) \equiv \int_{T_{\alpha-\Delta\alpha}}^{T_\alpha} \exp\left[\frac{-E_\alpha}{RT}\right]dT \quad (2),$$

β is the heating rate, and n is the number of the temperature programs. The highly accurate third order Senum-Yang approximation was used to compute the aforementioned integral, the relative error of approximation does not exceed 10^{-7} % for our particular case.[26] The GRG Nonlinear Solving method of Excel Solver add-in was used to determine a minimum of Equation (1). The uncertainties in the E_α values were evaluated according to procedure described in ref. [27].

The preexponential factor values were estimated by substituting the values of E_α into the equation of the compensation effect (3)

$$\ln A_\alpha = a + bE_\alpha \quad (3)$$

The parameters a and b were determined by fitting the pairs of $\ln A_i$ and E_i into Equation (3). The respective pairs were found by substituting the reaction models of F1, A4, A3, and A2 (Table 1), into the linear form of the basic rate equation (4):[21,28]

$$\ln\left(\frac{d\alpha}{dt}\right) - \ln[f_i(\alpha)] = \ln A_i - \frac{E_i}{RT} \quad (4)$$

Table 1. Some of the kinetic models used in the solid-state kinetics.

#	Code	$f(\alpha)$
1	P4	$4\alpha^{3/4}$
2	P3	$3\alpha^{2/3}$
3	P2	$2\alpha^{1/2}$
4	P2/3	$2/3\alpha^{-1/2}$
5	D1	$1/2\alpha^{-1}$
6	F1	$1-\alpha$
7	A4	$4(1-\alpha)[-\ln(1-\alpha)]^{3/4}$
8	A3	$3(1-\alpha)[-\ln(1-\alpha)]^{2/3}$
9	A2	$2(1-\alpha)[-\ln(1-\alpha)]^{1/2}$
10	D3	$3/2(1-\alpha)^{2/3}[1-(1-\alpha)^{1/3}]^{-1}$
11	R3	$3(1-\alpha)^{2/3}$
12	R2	$2(1-\alpha)^{1/2}$
13	D2	$[-\ln(1-\alpha)]^{-1}$

For each reaction model, $\ln A_i$ and E_i values were evaluated respectively from the slope and intercept of the linear plot of left-hand side of Equation (4) vs the reciprocal temperature.

Obtained sets of E_α and A_α values were further used for determination of the reaction model for the solid state polymerization of the synthesized cyanate ester. The reaction model was determined in the numerical form of Equation (5).[29,30]

$$g(\alpha) = \frac{1}{\beta}\sum_{\alpha} A_\alpha \int_{T_{\alpha-\Delta\alpha}}^{T_\alpha} exp\left(\frac{-E_\alpha}{RT}\right)dT \quad (5)$$

Results and discussion

It is well-known that polymerization of cyanate esters is a highly exothermic process leading to formation of cyanate (cyanurate, triazine) resins containing aromatic 1,3,5-triazine fragments as a cross-links. Thus, due to high exothermicity of the polymerization, the differential scanning calorimetry was chosen to investigate kinetics of the process (Figure 3). The absence of the endothermic signal of melting indicates the solid-state nature of the polymerization. In our case, the average reaction heat is 374±17 J g^{-1} (420±19 kJ mol^{-1}), which corresponds to 70±3 kJ per 1 mole of OCN group. The reaction heat values reported for other cyanate esters are typically lager varying in the range 80-110 kJ per 1 mole of OCN group.[17] A possible reason for lowering the reaction heat value is provided further.

View Article Online
DOI: 10.1039/D0PY00554A

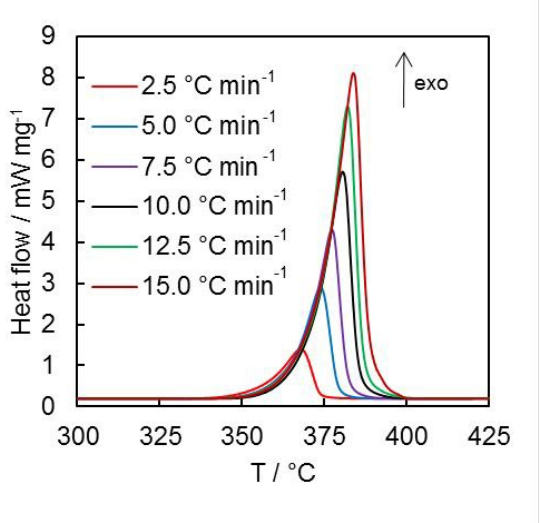

Figure 3. DSC curves of the cyanate ester 2 polymerization at different heating rates.

Fourier transform infrared (FTIR) spectroscopy shows the presence of characteristic absorption bands at 2265 and 2360 cm^{-1} (Figure 4) in synthesized monomer, which are attributed to stretching of cyanate group triple bond.[17] Their disappearance in the spectrum of the polymerization product (Figure 4) evidences that polymerization is complete. The FTIR spectrum of polymer also demonstrates the significant increase in absorption at 1360 and 1560 cm^{-1}, which corresponds to different modes of 1,3,5-triazine ring stretching. It should be noted that weak absorption band at 1360 cm^{-1} in monomer spectrum is attributed to complex O-C-N stretching vibration of cyanate group.[31,32]

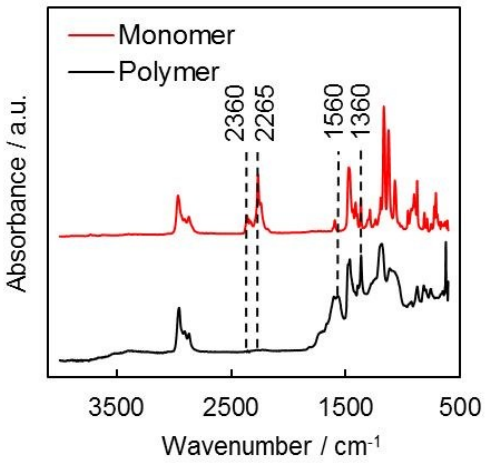

Figure 4. FTIR spectra of cyanate ester monomer and product of its polymerization.

The X-Ray powder diffraction (XRPD) analysis reveals crystallinity of monomer, but polymerization results in collapse of the crystal structure, so the polymer is in amorphous state (Figure 5).

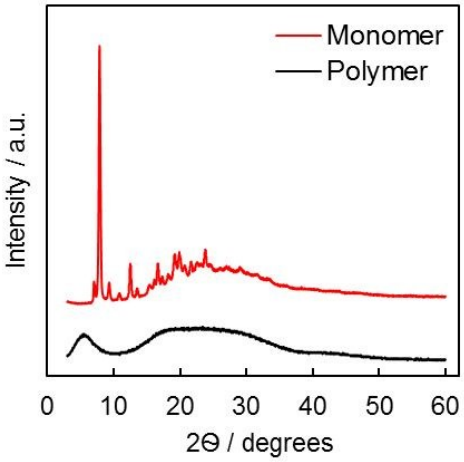

Figure 5. XRPD spectra of cyanate ester 2 and product of its polymerization.

The morphology of the synthesized cyanate ester **2** was studied by SEM that reveals plate-like crystals with well-defined faces and thickness of 7-10 μm (Figure S5 in SI).

The dependence of the effective activation energy (E_α) on the extent of conversion for polymerization is shown in Figure 6. It is seen that for this process E_α is practically independent of the extent of conversion below α = 0.8. After that the activation energy sharply drops to ~190 kJ mol^{-1}. The ratio of $[E_{\alpha(max)}-E_{\alpha(min)}]/E_{\alpha(average)}$ in aforementioned conversion range does not exceed 0.1 with an average value of activation energy equals to 380±10 kJ mol^{-1}. This constancy of the activation energy on the extent of conversion indicates that the kinetics of polymerization in that conversion range is likely to be determined by a single step.

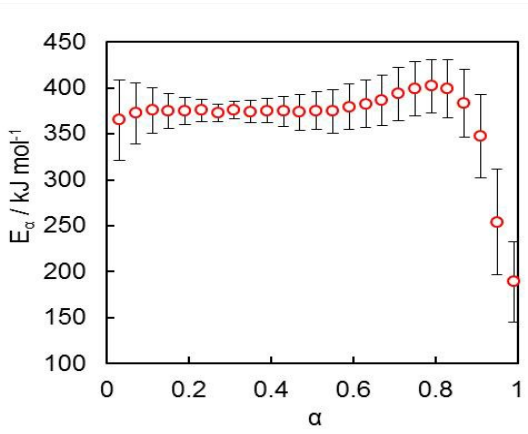

Figure 6. Activation energy as a function of conversion for solid-state polymerization of monomer.

The preexponential factor A is also nearly constant in the same region of conversions (Figure 7). Its averaged decimal logarithmic value equals to 28±1 (A in s^{-1}).

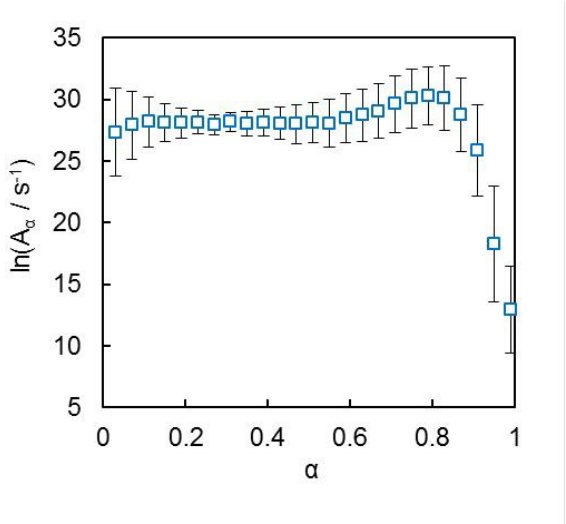

Figure 7. Preexponential factor A_α as a function of conversion for solid-state polymerization of monomer.

We assumed that drop of activation energy at high extent of conversion might be related to some degradation process accompanying polymerization. To check this idea we used simultaneous TG-DSC technique. Thermogravimetry reveals two mass loss steps (Figure 8). The first step is characterized by a minor mass loss of ca. 2-3%. It is encountered in the same temperature range as polymerization represented by a large exotherm. The second mass loss step is significantly larger and also partially overlaps with polymerization (Figure 8). We assign the minor mass loss to the monomer degradation, and the major mass loss to degradation of the polymer. Thermal stability of the obtained polymer is the same as for cyanate resins made of commercially available monomers. Peak mass loss rate of obtained polymer measured by TG at 10 °C min^{-1} is 488 °C, which is similar to that of other cyanate resins.[31]

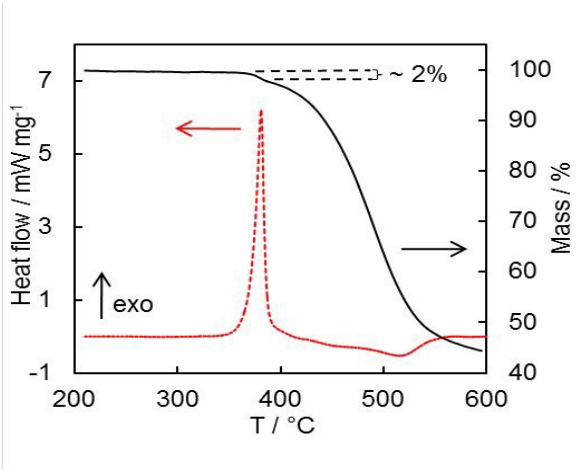

Figure 8. TG and DSC curves obtained in simultaneous TG-DSC run of monomer at 10 °C min^{-1}.

Mass-spectrometry of the gas released during the polymerization process confirms our assignment. The major signals at m/z = 56.1, 174.1 and 189.1 found in the mass-spectrum correspond to the structural fragments of the initial cyanate ester (Figure S6 in SI), which formed during monomer degradation process. An overlap of polymerization with degradation of monomer and polymer can explain the reason as to why the reaction heat for polymerization is somewhat smaller than for other cyanate esters. Processes of degradation of calix[n]arenes and cyanate resins in inert atmosphere are endothermic,[33,34] so that their occurrence simultaneously with exothermic polymerization should be expected to result in the overall reaction heat being smaller than the heat of polymerization. The results of effluent gas analysis allows us to suggest that degradation involves decyclization of cyanate ester molecules followed by consecutive aromatic fragments cleavage.[35]

It should be noted that acyclic analogues of the monomer must possess lower melting temperatures. For example cycloalkanes have higher melting and boiling temperatures compared to their acyclic counterparts due to more effective intermolecular interactions in condensed state, also acyclic analogue of 4-*tert*-butylcalix[6]arene has melting temperature of 250 °C,[36] while 4-*tert*-butylcalix[6]arene itself melts at 373 °C.[19] That means that acyclic products formed during degradation of the monomer may react in the liquid state.

Based on aforementioned reasoning we summarized possible reaction steps in a scheme that includes two competing channels (Figure 9). The first channel represents solid-state polymerization followed by degradation of the resulting polymer. The second channel includes degradation of the cyclic monomer to various acyclic products, which can then polymerize in the liquid state. The final step in this channel is also polymer degradation.

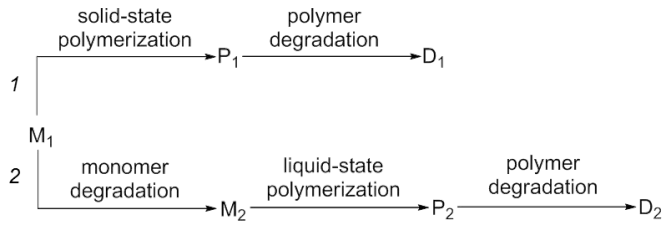

Figure 9. Proposed reaction scheme.

Generally, in the case of two competing reaction channels the effective activation energy increases between the values associated with the respective channels.[37] However, for our reaction system the activation energy is practically independent of conversion at $\alpha < 0.80$. This indicates that polymerization kinetics is limited by a single step with activation energy of 380±10 kJ mol^{-1}. It means that in the proposed reaction scheme

(Figure 9) one channel has a negligible effect on the overall kinetics. It is reasonable to assume that the second channel plays a negligible role. This channel includes three consecutive steps so that the activation energy for this channel cannot be larger than the activation energy of the individual steps. Degradation of the monomer (M_1) as well as the polymer (P_2) involves a C-C bond cleavage that in the condensed phase usually occurs in bimolecular fashion and, thus, has relatively low activation energy. For example, degradation of various polymers (e.g., polypropylene, polyethylene, polystyrene, polyvinylpyrrolidone, or phenol-formaldehyde resins) demonstrates the activation energy in the range of 70-250 kJ mol^{-1}.[38-40] Similarly, decomposition of calix[4]arene demonstrates the isoconversional activation energies that do not exceed 110 kJ mol^{-1}.[35] If the rate of this channel is limited by the liquid state polymerization of M_2 the activation energy of this channel should be comparable to that found for the liquid state polymerization of cyanate esters. The respective literature values reported for liquid-state polymerization of various neat cyanate monomers, including structurally-similar novolac-type cyanate ester, do not exceed 150 kJ mol^{-1}.[18,41-43] Therefore, it is highly unlikely for this channel to have activation energy as high as 380±10 kJ mol^{-1}.

On the other hand, such high activation energy is likely for the first channel that occurs as solid-state cyclization. This type of reaction is known to have very large activation energies. For example, solid state cyclization of L-leucyl-L-leucine into derivative of 2,5-piperazinedione possesses activation energy of 434±1 kJ mol^{-1} (logA = 48.0±0.1 (A in s^{-1})).[44] Even more reassuring example of the solid state cyclization is trimerization of sodium dicyanamide.[45] In this reaction the same 1,3,5-triazine fragment is formed, and kinetic parameters of the process are 373±71 kJ mol^{-1} and logA = 29±1 (A in s^{-1}).[45] Within the experimental error, these values are the same as for the presently studied solid-state polymerization of cyanate ester monomer (380±10 kJ mol^{-1} and logA = 28±1 (A in s^{-1}). Note that in both aforementioned cases the high values of the activation energy have been explained by cooperative bond breaking,[44,45] i.e., by simultaneously breaking more than one bond. It is, thus, reasonable to propose that the unusually high activation energy of presently studied solid-state polymerization is associated with the mechanism that involves cooperative bond breaking as the rate limiting step. Conversely, the liquid-state polymerization of cyanate esters is usually characterized by the activation energies that are about 3 times smaller, which is consistent with the mechanism comprising consecutive reaction of individual cyanate groups (Figure 1).

Thus, based on both literature and experimental evidence we can conclude that heating of the synthesized cyanate ester predominantly results in solid-state polymerization. In other words, the reaction scheme shown in Figure 9 can be reduced to the first channel. In this regard, we can also mention that a quick decrease in E_α from 380 to 190 kJ mol^{-1} at α>0.8 is consistent with a noticeable contribution of the polymer degradation at the final stages of high temperature polymerization.

It should be noted that sometimes solid-state reactions may actually include melting of the reactant that is immediately followed by a reaction with the formation of a solid product.[46] In this situation melting is strongly overlapped with reaction and, thus, might be impossible to detect by conventional DSC. To prove that the studied polymerization does indeed occur in the solid-state we have applied fast-scanning calorimetry (FSC). FSC is widely used for detecting of melting in highly reactive compounds. The approach makes use of the fact that with increasing the heating rate a chemical reaction shifts to higher temperatures, whereas melting does not. Onset of melting of the studied monomer was determined by FSC at the heating rates varying in the range 6 000 – 60 000 °C min^{-1}. As it turned out even the use of the slowest heating rate of 6 000 °C min^{-1} allows us to detect melting of the monomer without any sign of the exothermic polymerization (Figures S7 in SI). The absence of systematic variation in the onset melting temperature with the heating rate indicates that the results are not affected by the thermal lag (Figures S8 in SI). The averaged onset temperature of melting for our monomer is 403±1 °C, which is higher than the temperature range of polymerization (Figure 3). Therefore, we can confirm that the monomer cannot melt in the temperature range of polymerization so that polymerization does occur in the solid-state.

Next step of our study was to determine the reaction model of the rate limiting step of solid state polymerization of cyanate ester. The g(α) values of polymerization plotted against the theoretical g(α) models (Table 1) are shown in Figure 10. It is seen that none of these models fits the data well. It is also remarkable that g(α) has linear dependence on α, viz. g(α)=0.97α+0.06.

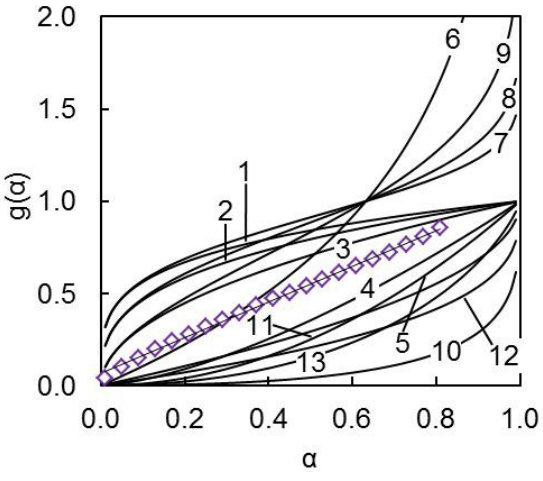

Figure 10. Dependencies of g(α) on the extent of conversion for the models listed in Table 1 (solid lines) and experimental g(α) data for solid state polymerization of the studied monomer (purple diamonds).

The existence of a linear dependence of g(α) on α means that the following holds true:

$$g(\alpha) \equiv \int_0^{\alpha} \frac{d\alpha}{f(\alpha)} = B\alpha + C \quad (6)$$

Differentiation of g(α) with respect to α leads to:

$$f(\alpha) = B^{-1} \equiv B^{-1}\alpha^{0} \quad (7)$$

Since B is constant, the reaction model f(α) and, thus, the process rate at constant temperature should be independent of α, as in the case of the so-called zero-order kinetics. Ideally, for zero-order kinetics, the value of B in eqn. 7 should be 1, rather than 0.97. However, one should keep in mind that g(α) has been determined experimentally by eq. 5 so that it contains an error due to the uncertainties associated with the experimental values of E_α and A_α.

The isothermal rate of polymerization has been measured at temperature of 338 °C. The results are displayed in Figure 11A along with the fit of experimental results to zero-order reaction model while using the values of E = 380 kJ mol^{-1} and log(A in s^{-1}) = 28.6 determined earlier. It is seen that the reaction rate indeed weakly depends on conversion in the range of α from 0.1 to 0.8. The corresponding α vs t_α curve shows linearity inherent to zero-order reaction model (Figure 11B).

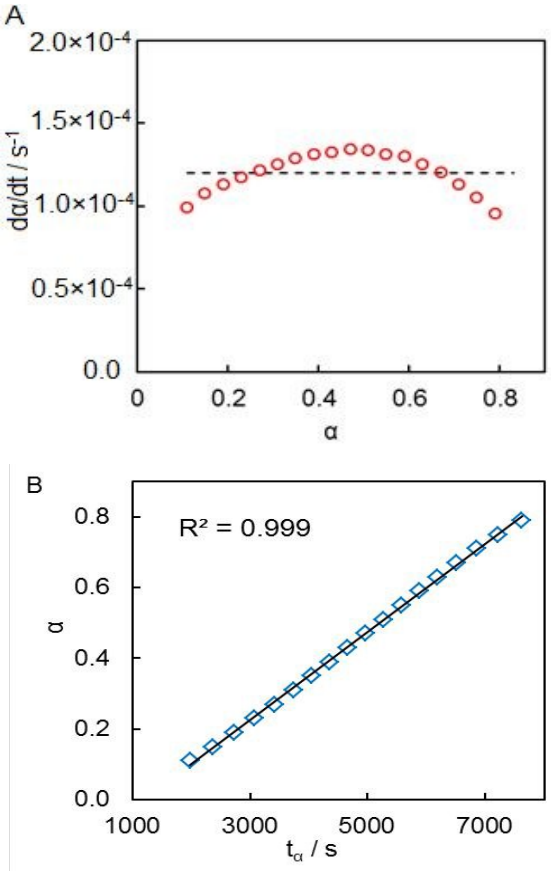

Figure 11. dα/dt vs α and α vs t_α plots for isothermal DSC runs of the cyanate ester **2** polymerization at 338 °C.

In chemical kinetics of homogeneous systems, the zero-order dependence of reaction rate on concentration of one of the reactants is typically observed in one of the two cases. The first case is when one of the reactants has significantly higher concentration than the other ones in reaction mixture. Then, the concentration of this reactant changes negligibly during the reaction so that the reaction rate is practically independent of this reactant concentration. Such situation can be illustrated by some enzymatic reactions, e.g., alcohol oxidation by liver alcohol dehydrogenase,[47] decomposition of phosphine on hot molybdenum filament,[48] tautomerization of vinyl alcohol catalyzed by trace amount of water.[49]

In the second case apparent zero-order kinetics originates from complex reaction mechanisms. For example zero-order dependence on the monomer concentration observed for polymerization of ε-caprolactone in presence of tin[50] or yttrium[51] compounds has been explained by the reaction mechanism that includes a slow rate-determining step of propagation proceeding in the coordination sphere of a metal complex followed by fast regeneration of this complex.[50] The same mechanism has been invoked to explain zero-order kinetics for ring-opening metathesis polymerization (ROMP) of norbornene catalyzed by titanacyclobutanes.[52] Likewise, ROMP catalyzed by third-generation Grubbs catalyst (G3), demonstrates zero-order kinetics because G3 dissociates releasing one equivalent of pyridine ligand, which inhibits polymerization and cancels out the catalyst concentration in the rate law so that the rate has zero-order dependence on the G3 concentration.[53]

Because all aforementioned cases apply to reactions that include at least two reactants, none of the respective explanations can be used to understand the origins of zero-order kinetics in the presently studied single reactant polymerization of cyanate ester. In this circumstance, an explanation should be sought in the solid-state nature of the reaction. In general, reactions of solids are topochemical,[46] which means that the reaction front is localized at the interface between the solid reactant and a product that can be in the solid or another aggregate state. The topochemical kinetics are quite complex and, thus, give rise to a broad variety or reaction models, some of which are listed in Table 1. The reaction order type of models (R2, R3) represent the situation when the reaction centres (nuclei of the product phase) are formed rapidly and extensively throughout all solid surfaces. Then the rate is controlled by the growth of the product phase or the contraction of the solid reactant. Depending on the dimensionality of the reacting solid contraction the reaction order takes on different numerical values of n. The 3D contraction (contracting sphere) is represented by n=2/3, the 2D contraction (contracting cylinder) by n=1/2, and 1D contraction by n=0.53 Zero-order kinetics are not common in the topochemical reactions. Yet, a number of cases is documented.[54] One such case is the reaction on the surface of

the thin plate crystals, i.e., crystals of the shape similar to that seen for the present cyanate ester (Figure S5).

In such structures, the lateral surface area is markedly smaller than the area of the top and bottom surfaces. Since the rate of a topochemical reaction is proportional to the surface area, the contraction of a plate-like crystal should occur primary in the direction perpendicular to the top and bottom surfaces, i.e., in one dimension (Figure 12).

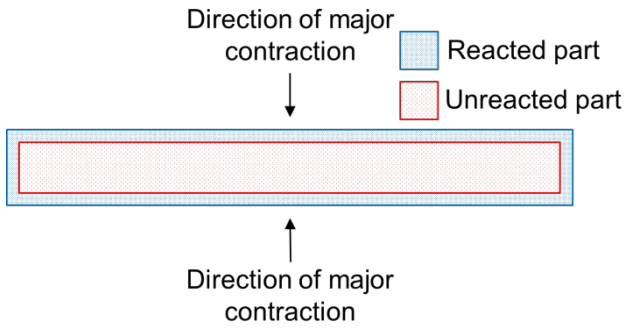

Figure 12. Propagation of reaction fronts in a plate-like crystal of the monomer (cross-section).

Thus, zero-order kinetics, i.e., independence of the reaction rate of the extent of conversion, arises from the fact that throughout the most of reaction the area of the top and bottom surfaces undergoes little change. As a result, the rate remains nearly constant in a broad range of conversions.

Conclusions

We have synthesized a unique cyanate ester monomer based on 4-*tert*-butylcalix[6]arene that undergoes thermally induced polymerization in the solid state. The kinetics of the solid-state polymerization studied by DSC has demonstrated unusually high activation energy of 380±10 kJ mol^{-1} testifying that the rate limiting step of the process involves cooperative breaking of C≡N bonds. This is in contrast to the regular cyanate esters that polymerize in the liquid-state and demonstrate the activation energies that are about three times smaller and, thus, representative of consecutive breaking of C≡N bonds. Kinetic analysis has also revealed that polymerization follows zero-order reaction model, i.e., the rate of polymerization is independent of the amount of monomer. This has been explained by the topochemical nature of polymerization, which is localized on the surface of plate-like crystals of the monomer. The independence of the rate on the monomer amount, therefore, arises from the fact that there is significantly more monomer present on the top and bottom surfaces of the crystal than on its lateral surfaces. Since the rate of a topochemical reaction is proportional to the surface area, the reaction front in a plate-like crystal moves primarily in the dimension parallel to the lateral surface so that the area of the top and bottom surfaces does not change much, making the polymerization rate practically independent of conversion.

Conflicts of interest

View Article Online
DOI: 10.1039/D0PY00554A

There are no conflicts to declare.

Acknowledgements

This research was conducted with a support of the Russian Science Foundation (Project № 19-73-10148).

References

1 A. Matsumoto and T. Tanaka, *Mol. Cryst. Liq. Cryst*., 2005, **440**, 215–222.
2 M. Ikeshima, H. Katagiri, W. Fujiwara, S. Tokito and S. Okada, *Cryst. Growth Des*., 2018, **18**, 5991–6000.
3 G. W. Oakley, S. E. Lehman, J. A. Smith, P. Van Gerven and K. B. Wagener, *Macromolecules*, 2003, **36**, 539–542.
4 M. Hasegawa, *Pure. Appl. Chem*., 1986, **58**, 1179–1188.
5 H. Matsuzawa, S. Okada, A. Sarkar, H. Matsuda and H. Nakanishi, *Polymer Journal*, 2001, **33**, 182-189.
6 M. Kamath, W. H. Kim, L. Li, J. Kumar and S. Tripathy, Macromolecules, 1993, 26 (22), 5954–5958.
7 R. R. Chance and G. N. Patel, *J Polym. Sci. Polym. Phys. Ed*., 1978, **16**, 859–881.
8 C. Shi, S. M. Gross, J. M. DeSimone, D. J. Kiserow and G. W. Roberts, *Macromolecules*, 2001, **34**, 2060–2064.
9 M. A. G. Jansen, J. G. P. Goossens, G. De Wit, C. Bailly, C. Schick and C. E. Koning, *Macromolecules*, 2005, **38**, 10658–10666.
10 V. S. Iyer, J. C. Sehra, K. Ravindranath and S. Sivaram, *Macromolecules*, 1993, **26**, 1186-1187.
11 S. M. Gross, G. W. Roberts, D. J. Kiserow and J. M. Desimone, *Macromolecules*, 2001, **34**, 3916–3920.
12 N. Kasmi, Z. Terzopoulou, G. Z. Papageorgiou, D. N. Bikiaris, *EXPRESS Polym. Lett*., 2018, **12**, 227–237.
13 S. N. Vouyiouka, E. K. Karakatsani and C. D. Papaspyrides, *Prog. Polym. Sci.*, 2005, **30**, 10–37.
14 F. Guo, J. Martı´-Rujas, Zh. Pan, C. Hughes and K. Harris, *J. Phys. Chem. C*, 2008, **112**, 19793-19796.
15 V. Enkelmann, *Advances in Polymer Science* Ed. Springer: Berlin, 1984, **63**, 91-136.
16 L. R. MacGillivray, J. L. Atwood, J. W. Steed and G. S. Papaefstathiou, In *Encyclopedia of supramolecular chemistry* Eds. Marcel Dekker Inc.: New York, 2004, 1316-1319.
17 I. Hamerton, *Chemistry and Technology of Cyanate Ester Resins*, Chapman & Hall: Glasgow, 1994.
18 S. L. Simon and J. K. Gillham, *J. Appl. Polym. Sci*., 1993, **47**, 461–485.
19 C. D. Gutsche, *J. Am. Chem. Soc.*, 1981, **103**, 3782–3792.
20 S. Vyazovkin, *Isoconversional Kinetics of Thermally Stimulated Processes*, Springer: Switzerland, 2015.
21 S. Vyazovkin, A. K. Burnham, J. M. Criado, L. A. Pérez-Maqueda, C. Popescu and N. Sbirrazzuoli, *Thermochim. Acta*, 2011, **520**, 1–19.
22 S. Vyazovkin and D. Dollimore, *J. Chem. Inf. Comput. Sci*., 1996, **36**, 42-45.
23 S. Vyazovkin, *J. Comput. Chem*., 1997, **18**, 393–402.
24 S. Vyazovkin, *J. Comput. Chem*., 2001, **22**, 178-183.
25 S. Vyazovkin, N. Koga and S. Christoph, *Handbook of Thermal Analysis and Calorimetry*, Eds. Elsevier, 2018, 131-172.
26 G. I. Senum, R. T. Yang, *J. Therm. Anal*., 1977, **11**, 445–447.
27 S. Vyazovkin, C. A. White, *Anal. Chem*., 2000, **72**, 3171-3175.
28 Sbirrazzuoli, N. *Thermochim. Acta*, 2013, **564**, 59-69.
29 S. Vyazovkin, I. Dranca, X. W. Fan and R. Advincula, *Macromol. Rapid Commun*., 2004, **25**, 498-503.
30 S. Vyazovkin, *Int. J. Chem. Kinet*., 1996, **28**, 95-101.

View Article Online
DOI: 10.1039/D0PY00554A

31 M. L. Ramirez, R. Walters, R. E. Lyon and E. P. Savitski, *Polym. Degrad. Stabil*. 2002, **78**, 73-82.
32 S. Rakesh and M. Sarojadevi, *Chem. Chem. Technol*. 2008, **2**, 239–247.
33 A. Saponar, E. J. Popovici, I. Perhaita, G. Nemes and A. I. Cadis, *J. Therm. Anal. Calorim*., 2012, **110**, 349-356.
34 L. Eddaif, L. Trif, J. Telegdi, O. Egyed, A. Shaban, *J. Therm. Anal. Calorim.*, 2019, **137**, 529–541.
35 K. Chennakesavulu, M. R. Basariya, P. Sreedevi, G. Bhaskar Raju, S. Prabhakar and S. S. Rao, *Thermochim. Acta*, 2011, **515**, 24–31.
36 G. Casiraghi, M. Cornia, G. Ricci, G. Balduzzi, G. Casnati and G. D. Andreetti, *Die Makromolekulare Chemie*, 1983, **184**, 1363-1378.
37 S. Vyazovkin, *Phys. Chem. Chem. Phys*., 2016, **18**, 18643-18656.
38 J. D. Peterson, S. Vyazovkin and C. A. Wight, *Macromol. Chem. Phys.*, 2001, **202**, 775–784.
39 A. E. Jablonski, A. J. Lang and S. Vyazovkin, *Thermochim. Acta*, 2008, **474**, 78–80.
40 B. D. Park, J. F. Kadla, *Thermochim. Acta*, 2012, **540**, 107-115.
41 C. C. Chen, T. M. Don, T. H. Lin and L. P. Cheng, *J. Appl. Polym. Sci.*, 2004, **92**, 3067-3079.
42 A. Galukhin, T. Liavitskaya and S. Vyazovkin, *Macromol. Chem. Phys.*, 2019, **220**, 1–8.
43 A. Osei-Owusu, G. C. Martin and J. T. Gotro, *Polym. Eng. Sci*., 1992, **32**, 535–541.
44 M. A. Ziganshin, A. S. Safiullina, A. V. Gerasimov, S. A. Ziganshina, A. E. Klimovitskii, K. R. Khayarov and V. V. Gorbatchuk, *J. Phys. Chem. B*, 2017, **121**, 8603–8610.
45 B. Yancey and S. Vyazovkin, *Phys. Chem. Chem. Phys*., 2014, **16**, 11409–11416.
46 F. Toda, Ed. *Organic Solid-State Reactions*, Springer: Netherlands, 2002.
47 I. Tinoco, K. Sauer, J. Wang, J. Puglisi, G. Harbison and D. Rovnyak, *Physical chemistry: principles and applications in biological sciences*, 5th edition Pearson: 2014.
48 H. Melville and H. Roxburgh, *J. Chem. Soc*., 1933, 586-595.
49 B. M. Novak and A. K. Cederstav, *J. Macromol. Sci*., *Part A. – Pure Appl. Chem*., 1997, **34**, 1815–1825.
50 M. B. Bassi, A. B. Padias and H. K. Hall, *Polym. Bull*., 1990, **24**, 227–232.
51 B. M. Chamberlain, B. A. Jazdzewski, M. Pink, M. A. Hillmyer and W. B. Tolman, *Macromolecules*, 2000, **33**, 3970–3977.
52 L. R. Gilliom and R. H. Grubbs, *J. Am. Chem. Soc*., 1986, **108**, 733–742.
53 D. J. Walsh, S. H. Lau, M. G. Hyatt and D. Guironnet, *J. Am. Chem. Soc*., 2017, **139**, 13644–13647.
54 M. Brown, D. Dollimore, A. Galwey, Eds. *Reactions in the solid state*, Elsevier: Netherlands, 1980.

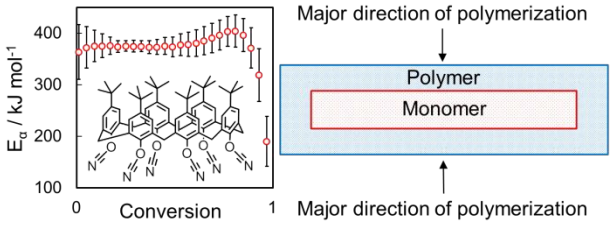

View Article Online
DOI: 10.1039/D0PY00554A

Solid-state polymerization of cyclic cyanate ester shows zero-order kinetics and proceeds through cooperative breaking of C≡N bonds.